A cucurbit[8]uril-based probe for the detection of the pesticide tricyclazole

Heng Wu,[a] Jie Zhao,[a] Xi Nan Yang,[a] Dan Yang,[a] Li Xia Chen,[a] Carl Redshaw,[b] Zhu Tao [a] and Xin Xiao*[a]

[a] Key Laboratory of Macrocyclic and Supramolecular Chemistry of Guizhou Province, Guizhou University, Guiyang 550025, China.

[b] Department of Chemistry, University of Hull, Hull HU6 7RX, U.K.

E-mail: gyhxxiaoxin@163.com (X. Xiao)

Abstract

A system comprising cucurbit[8]uril (Q[8]) and a fluorescent molecule HPy has been utilized to construct a fluorescent probe that is capable of detecting the pesticide tricyclazole (TC). A variety of techniques including ^{1}H NMR spectroscopy together with fluorescence experiments have been employed to investigate the host-guest properties of the Q[8]/HPy system in aqueous solution. Results indicate that the system forms the stable 2:1 inclusion complex HPy_2@Q[8], and that this inclusion complex imparts fluorescent quenching on HPy. The addition of a number of pesticides was found to have no obvious effect on the fluorescence, however on addition of tricycazole (TC), the fluorescence intensity underwent a dramatic enhancement. The linear relationship between the fluorescence intensity and the concentration of TC allowed for the facile

detection of TC concentration in aqueous target solutions as well as in agricultural products. The detection limit was found to be 3.70×10^{-8} mol·L^{-1}.

Keywords: Cucurbit[8]uril, host-guest chemistry, fluorescent probe, pesticide detection.

1.Introduction

To maximize the production of crops, pesticides are frequently employed in order to control the levels of unwanted pests and diseases. Whilst this is beneficial for the agricultural economy, the use of pesticides can have detrimental side effects on both the wider environment as well as on human health.[1,2] With this in mind, there is a need for simple yet sensitive analytical methods capable of the rapid detection and quantification of specific pesticide residues. Methods employed to date include mass spectrometry (MS),[3] gas chromatography (GC),[4] high performance liquid chromatography (HPLC),[5] fluorescence spectrophotometry,[6,7] and ultraviolet-visible spectrophotometry.[8,9] It is worth noting that fluorescent probes have many advantageous characteristics such as excellent selectivity, high sensitivity and fast response times, which makes them useful for the real-time detection of small molecules and ions.[10-16] Research efforts continue at a pace to try and develop effective fluorescent probes for pesticide detection.

Tricyclazole (5-methyl-1,2,4-triazolo[3,4-b]benzothiazole) is a pervasive fungicide that is employed as an effective control of rice blast disease.[17] Its widespread application means that it is present in soil, water and vegetation, and this has led to investigations into its subsequent fate.[18,19] The combination of its stability in water/soil systems,[20] together with its mutagenic and carcinogenic properties has led to its classification by the WHO as a moderately hazardous pesticide.[21] This has driven the search for analytical methods capable of measuring tricyclazole concentrations in aquatic environments. Much work on fluorescent probes over the last decade or

so has relied on the use of macrocyclic hosts in combination with dyes to detect organic analytes.[22-30] Such systems rely on the change in the fluorescence, be it quenching or enhancement, upon competitive encapsulation of the dye and analyte by the macrocycle.

Chemists have synthesized many intriguing macrocycles over the years, and one of the more recent additions are the cucurbit[*n*]uril family (*n* = 5-8, 10, 13-15, often abbreviated as Q[*n*]s). Q[*n*]s possess a hydrophobic cavity and a carbonyl-laced portal, and have been widely employed in fluorescent probes and for molecular recognition.[31-41] In particular, Q[*n*]s have recently been exploited in fluorescent probes for the detection of organic analytes, as reported by Nau and Biedermann *et al*. for the detection of steroids.[42] For pesticide detection, the reported fluorescent probe systems based on Q[*n*]s are typically used to detect paraquat.[43-46] Recently, our research group constructed two fluorescent probe systems based on Q[10] to detect the pesticide dodine.[47,48] In order to develop probes for detecting other pesticides, we selected 17 pesticides for one-by-one detection. We note that reports on tricyclazole detection by a fluorescent Q[8] probe system have not appeared in the literature.

Herein, we have designed the fluorescent molecule (E)-1-(2-hydroxyethyl)-4-(4-hydroxystyryl)pyridin-1-ium bromide (abbreviated as HPy, see Scheme 1), and have employed it in conjunction with Q[8] for the detection of the pesticide tricyclazole. ^{1}H NMR and fluorescence spectroscopies have been employed to study the binding properties of the system, and the results were consistent with the formation of a 1:2 complex. The system displays fluorescence of moderate intensity, which was greatly enhanced upon addition of tricyclazole (TC). It is noteworthy here that the addition of other pesticides to the same complex fails to change the fluorescence. Thus, this system is capable of the selective identification of TC in aqueous solution.

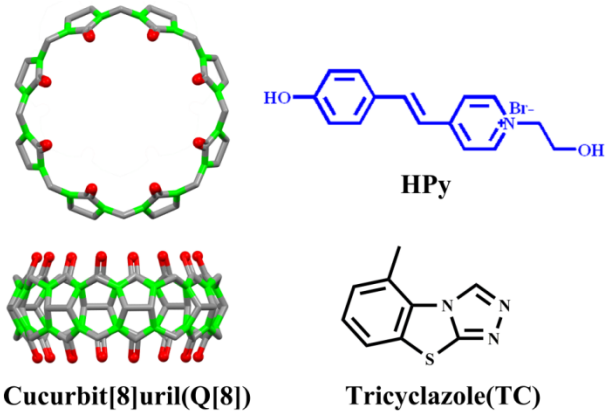

Scheme 1. Structural representations of Q[8], HPy and TC.

2.Experimental section

Instruments. Fluorescence data were recorded on a Varian RF-540 fluorescence spectrophotometer at 293.15 K, whilst NMR spectroscopic data were recorded on a JEOL JMM-ECZ400 spectrometer in D_2O (pD = 4.0).

Reagents and Chemicals. The synthetic method for HPy is provided in the Supporting Information (Figure S1-S3). In the laboratory, the relevant preparation of Q[8] was completed by using the literature method.[49] All pesticides used were obtained from commercial sources, and further purification was not necessary. Stock solutions of pesticides (1×10^{-3} mol·L^{-1}), HPy (1×10^{-3} mol·L^{-1}) and Q[8] (1×10^{-4} mol·L^{-1}) were prepared using double-distilled water. In addition, a variety of pesticides have been employed herein including Propiconazole(PPZ), Tebuconazole(TBZ), Dinotefuran(DFA), Tricyclazole(TC), Azaconazole(ACZ), Metalaxyl(MTL), Triadimefon(TDF), Pymetrozine(PTZ), Pyroquilon(PQL), Flusilazole(FSZ),

Triadimenol(TDO), Acetamiprid(ATM), Flutriafol(FTO), Pyrimethanil(PMA), Thiamethoxam(TTA), Penconazole(PCZ) and Hymexazol(HMZ) (the structures of the 17 pesticides are shown in Fig. S4). The preparation process of the solutions employed herein was to dilute the stock solution to obtain the corresponding concentration standard. This involved initially storing the stock standard solution at room temperature for several weeks prior to use. When preparing the standard working solution, double distilled water was gradually dropped into the stock standard solution. All other chemicals were of analytical reagent grade. The extracts of yam, cabbage, nectarine and capsicum frutescens were provided by the Guiyang Quality Inspection Base of the National Quality Inspection Center.

^{1}H NMR spectroscopic measurements. Experiments were recorded at 25 ℃, using a JEOL JMM-ECZ400 spectrometer with D_2O as the field frequency lock. The observed chemical shift is reported in parts per million (ppm) relative to the built-in tetramethylsilane (TMS) standard (0.0 ppm).

The detection limits (LOD) measurement. The calculation technique used for the LOD was based on the standard derivation of 10 measurements without the guest molecule (σ) and the slope of the linear calibration curve (K) based on the formula LOD = 3σ/K. In the absence of guest molecules, the standard deviation for 10 measurements can be deduced using: $\sigma = \sqrt{\frac{1}{n-1}\sum_{i=1}^{n}(x_i - \bar{x})^2}$, where n is 11 measurements (the relevant data is shown in Table S3).

Measurement of fluorescence spectra. HPy of concentration 2×10^{-5} mol·L^{-1} was obtained by diluting the stock solution. A certain proportion of Q[8] solution was gradually added to free HPy. The maximum emission wavelength (λem) of the sample is 510 nm, and the excitation wavelength (λex) is 376 nm. HPy_2@Q[8] has a bandwidth of 5 nm for the emission and excitation.

To the aqueous solutions of the HPy_2@Q[8] inclusion complex (4×10^{-6} mol·L^{-1}), a known amount of pesticide solution was gradually added in proportions. Fluorescence spectra were

obtained upon excitation at 376 nm (emission and excitation bandwidths: 5 nm), at room temperature, and the emission intensity was monitored at 510 nm.

A known amount of tricyclazole solution was added to the extract sample, followed by an aqueous solution of the HPy_2@Q[8] (4×10^{-6} mol·L^{-1}). Simultaneously, at room temperature, the emission intensity data was monitored at 510 nm (excitation and emission bandwidth of 5 nm).

3. Result and discussion

3.1. NMR spectroscopic analysis

The use of NMR spectroscopy is central to the investigation of host-guest interactions. The technique has been employed herein to provide information about the interaction between Q[8] and HPy. Displayed in Fig. 1 are the ^{1}H NMR spectra of the free guest HPy (see A), Q[8]/ HPy with ratio 1:2 (see B), and at the bottom (C) the ^{1}H NMR spectrum of Q[8]. It is evident from these results that, when in the presence of Q[8], specific protons of HPy, specifically Ha, Hb, Hc, Hd, He, Hf and the methylene proton Hg undergo significant upfield shifts from δ 6.82, 7.52, 7.06, 7.64,7.86,8.42 and 4.43 to 6.12, 6.78, 5.89, 6.46, 6.94,7.99 and 4.40, respectively. Spectrum B also reveals that the proton Hh of HPy are slightly shifted downfield. These results indicate that HPy has been inserted into the Q[8] cavity, thereby forming HPy_2@Q[8] (for the COSY NMR spectrum of HPy_2@Q[8] see Fig. S5). Furthermore, the mass spectrometry results provide strong support (Fig. S6); the mass spectrum displayed a signal at m/z = 906.31, corresponding to the molecular ion $[HPy_2@Q[8]-2Br^-]^{2+}$ (calculated: 906.31).

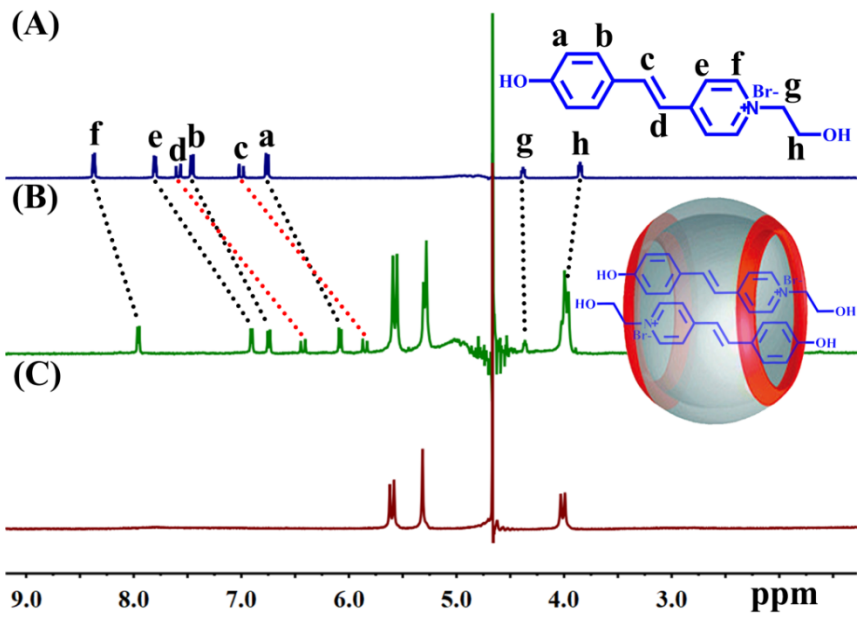

Figure 1. ^{1}H NMR spectra (400 MHz, D_2O) of free HPy (A), HPy_2@Q[8] (B) and free Q[8] (C).

3.2. Fluorescence emission spectra

To further understand the mole ratio of the interaction between Q[8] and HPy, fluorescence spectroscopy experiments were conducted. As shown in Fig. 2, the strong green fluorescence at λ_{max} 510 nm exhibited by HPy (2×10^{-5} mol·L^{-1}) in aqueous solution (Fig. 2A) is significantly weakened on gradual addition of Q[8] until a 1:2 (ratio Q[8]/HPy) is achieved (Fig. 2B). This result is consistent with the formation of the species HPy_2@Q[8], which was further verified by a Job's plot (Fig. 2C), for which the maximum peak appeared at a mole fraction of 0.33, corresponding to a 1:2 binding stoichiometry for Q[8] to HPy. Adding Q[8] to a HPy aqueous solution leads to fluorescence quenching, which may be attributed to charge transfer between Q[8] and HPy.

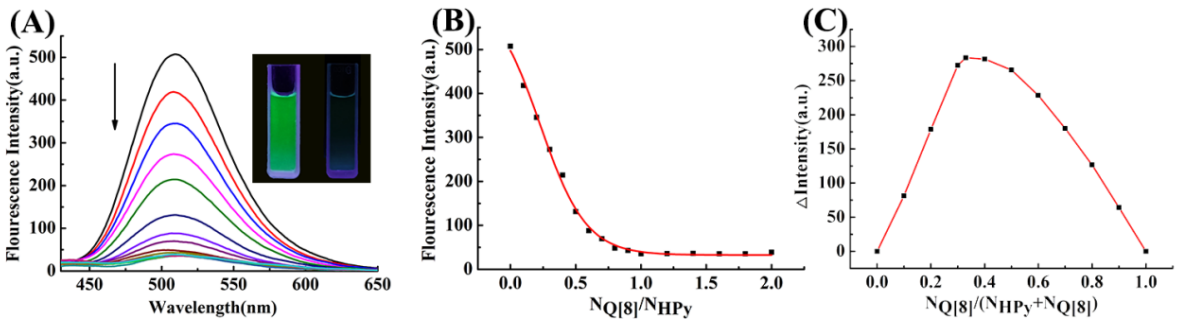

Figure 2. (A) Fluorescence spectra (λ_{ex} = 376 nm) of HPy (2.0×10^{-5}mol/L) on increasing Q[8] concentration (0, 0.1, 0.2……0.8, 0.9, 1.0 equiv.); (B) the corresponding F *vs*. $N_{Q[8]}/N_{HPy}$ curves; (C) the Job's plot.

3.3. Fluorescence regeneration of HPy_2@Q[8] by TC

As mentioned above, a non-fluorescent host-guest system allows us to think about whether it might be applied for analytical detection. This can be achieved by designing it so that it is capable of 'turning-on' fluorescence, for example to detect pesticides. To evaluate if the system HPy_2@Q[8] could indeed be utilized as a pesticide sensor and for monitoring the concentration thereof, seventeen pesticides (Fig. 3) were screened using a solution of the HPy_2@Q[8] inclusion complex (4.0×10^{-6} mol·L^{-1}). In the case of the fluorescence emission of HPy, the emission continuously recovers on increasing the TC concentration. By contrast, the addition of any of the other 16 pesticides under the same conditions (*i.e*. addition to a HPy_2@Q[8] aqueous solution of the same concentration) failed to result in a significant increase in fluorescence. Such observations suggest that the inclusion complex HPy_2@Q[8] does have the potential to be employed for the selective recognition of TC when employed in aqueous solution.

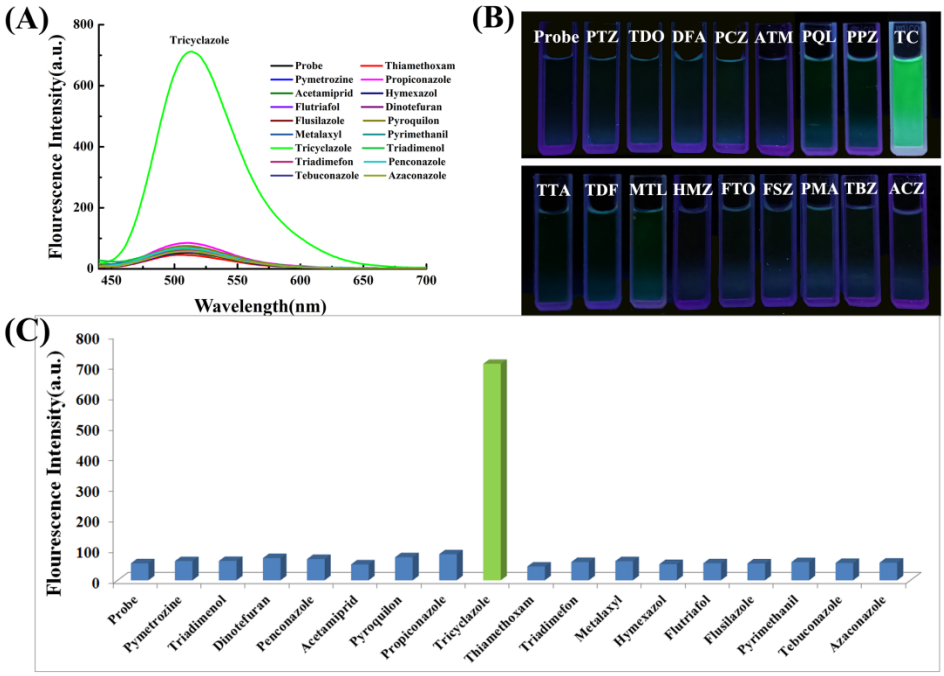

146

147 **Figure 3.** (A) The impact of the 17 pesticides (1.0 equiv. of host-guest complex) on the respective
148 fluorescent response (λ_{max} em = 510 nm) of HPy_2@Q[8] (4.0×10^{-6} mol·L^{-1}) (2:1); (B) Photographs
149 showing the HPy_2@Q[8] systems containing 1 equiv. of host-guest complex and 17 different
150 pesticides when exposed to UV light (365 nm) ; (C) The impact of the 17 pesticides (1 equiv. of
151 host-guest complex) on the relative fluorescence intensity (λ_{em} = 510 nm) of HPy_2@Q[8] (4.0×10^{-6}
152 mol·L^{-1}) (2:1).

153

154 More interestingly, the fluorescence intensity of the system is much higher than that of free
155 HPy when 1 equivalent of TC solution is added, and adding TC to the free HPy solution does not
156 cause the changes of fluorescence intensity (Fig. S12). The fluorescent changes on gradually
157 adding TC to the probe were then studied, see Fig. 4. It can be seen that the intensity initially
158 increases as the TC is added before eventually flattening off (the non-linear fitting is shown in Fig
159 S10). The initial enhancement is linear (Fig. 4B), with a linear regression equation of ΔI =
160 216.15C+35.53 (R^2 = 0.99113, C denotes the TC concentration). The detection limit for the TC

was determined to be 3.70×10^{-8} mol·L^{-1}. The linear range was 4×10^{-5}~2.4×10^{-6} mol·L^{-1}. Such a trend means that the fluorescence intensity can be used both for the quantification and detection of TC residues. The selectivity of the probe is good, given that none of the other pesticides employed herein caused any significant interference (Fig. 5. The relevant fluorescence spectrum is shown in Fig. S13).

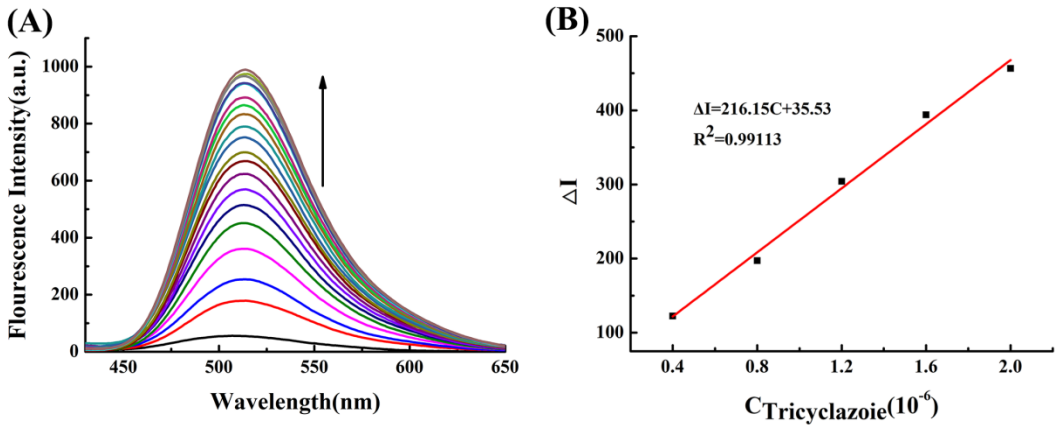

Figure 4. (A) The titration fluorescence spectra for HPy_2@Q[8] (4.0×10^{-6} mol·L^{-1}) on increasing TC concentration (0, 0.1, 0.2……1.8, 2.0 equiv. of host-guest complex, the maximum volume of dripping to 24 μl TC); (B) Linear fitting curves for the changes in the fluorescence intensity for the complex *versus* different concentrations of TC.

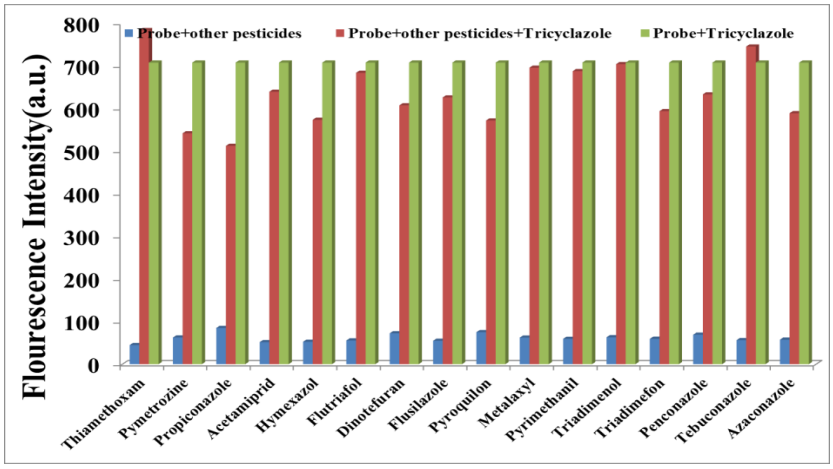

Figure 5. The effect of binary mixtures of TC (4.0×10^{-6} mol·L^{-1}) and other pesticides (4.0×10^{-6} mol·L^{-1}) on the fluorescence of HPy_2@Q[8] (4.0×10^{-6} mol·L^{-1}).

3.4. Fluorescence turn-on mechanism

In order to gain insight into the mechanism operating when the fluorescence is enhanced upon addition of TC to the inclusion complex HPy_2@Q[8], ^{1}H NMR spectroscopic studies were conducted. The results revealed that the protons associated with TC underwent an upfield shift (*versus* free TC), consistent with TC encapsulation by the Q[8] cavity (Fig. 6). Concomitantly, a shift to lower field (*versus* HPy_2@Q[8]) was observed for the protons Ha, Hb, Hc, Hd, He, Hf and the methylene proton Hg of HPy. Some protons of HPy have returned to the free state (black dotted line in Fig. 6C), and some remain at a higher field (red dashed line in Fig. 6C) relative to free HPy. Such observations demonstrate that one included HPy molecule is displaced by the TC molecule. The result is that both HPy and TC simultaneously bind within the Q[8] cavity, *i.e*. formation of a 1:1:1 complex (the mass spectrum is given in Fig. S11). Subsequently, the interaction between TC and Q[8] was studied by UV-Vis spectroscopy (see Fig. S8) and isothermal titration calorimetry (see Fig. S9) experiments. Indeed, the ITC experiment revealed that the binding constant K_a of TC@Q[8] is higher than that the second binding constant K_{a2} of HPy_2@Q[8], but is comparable to the first binding constant K_{a1} (see Fig.S7), which would explain why a bound HPy molecule is replaced by a TC.

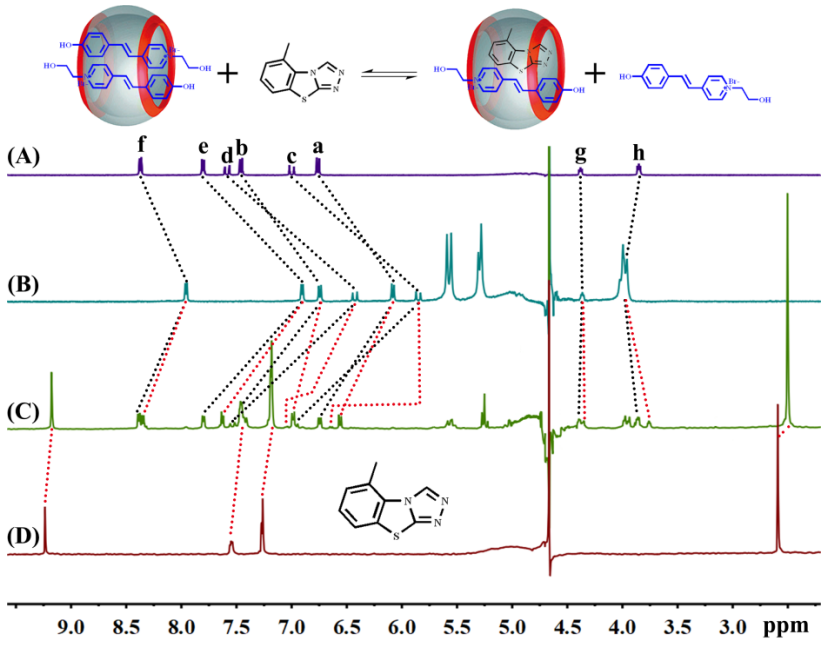

Figure 6. ^{1}H NMR spectra (400 MHz, D_2O) of free HPy (A), HPy_2@Q[8] (B), TC@HPy@Q[8] (C) and free TC (D).

Based on the ^{1}H NMR spectra, a semiempirical computational model was constructed via use of the fast tight-binding quantum chemical method GFN2-xTB, as implemented in the xtb 4.8 stand-alone program, see Fig. 7 and S15. The model for TC@HPy@Q[8] reveals that the TC forms a π-π interaction with HPy (binding energy = −49.4 kcal·mol^{-1}), and it becomes apparent that when compared to HPy_2@Q[8] (binding energy = −46.1 kcal·mol^{-1}), the tertiary complex TC@HPy@Q[8] exhibits enhanced stability. It can therefore be surmised from these results that greater fluorescent enhancement is achieved from the stable inclusion complex, whilst the inability of the other 16 pesticides to replace HPy means they afford no fluorescence variation.

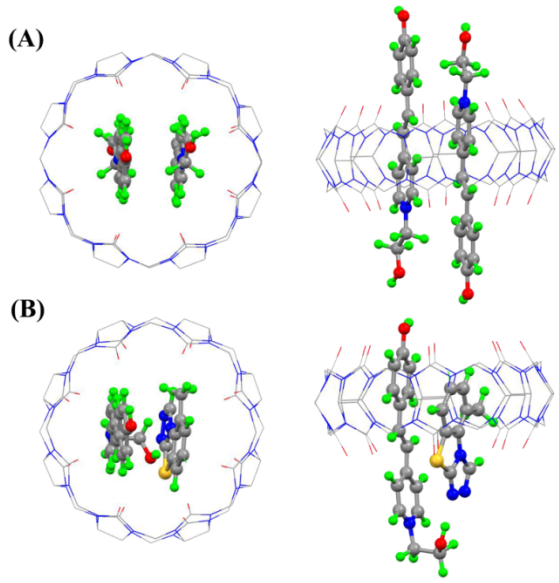

Figure 7. (A) Semiempirical model of the ternary inclusion complex HPy_2@Q[8]; (B) Semiempirical model of the ternary inclusion complex TC@HPy@Q[8].

3.5. Detection of TC in real vegetables samples

We have attempted to utilize the system developed herein in more applied settings, namely for the detection of the level of the TC residue in rice leaves in local farmland. Given that no TC residues were found in the rice leaf samples, a different approach was taken, whereby dilute TC of differing concentration was smeared over the surface of rice leaf. On adding the fluorescence probe solution, fluorescence signals of differing intensities were observed (Fig. 8) under UV light. The different intensities are associated with the respective TC concentrations, and this suggests that this probe can be employed for the detection of TC residues in real agricultural products.

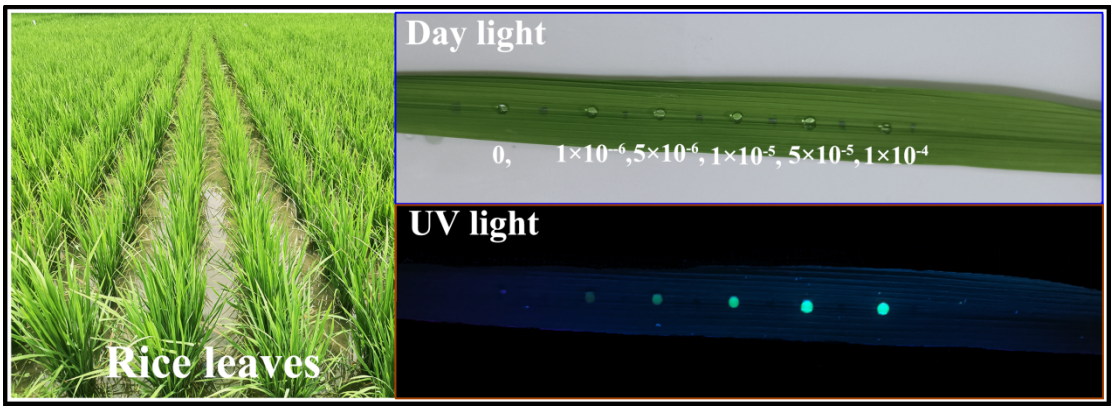

Figure 8. Rice leaf smeared with solutions containing different concentrations of TC to simulate pesticide residue.

These studies were then extended to the attempted detection of TC residues in extracts of yam, cabbage, nectarine and sweet pepper. Different concentrations of tricyclazole solutions were added to each of the extracts of yam, cabbage, nectarine and capsicum frutescens, followed by addition of the fluorescence probe solution (see Fig. 9). Under a 365 nm UV light, the fluorescence intensity of the system is seen to increase with increasing tricyclazole concentration. Subsequently, we once again added different concentrations of tricyclazole and the same concentration of probe solution to each extraction solution and performed fluorescence spectroscopy experiments. The results are shown in Fig. S14. In each extract, an increase in fluorescence emission intensity was observed as the concentration of tricyclazole increased. This again suggests that the system has potential application for TC detection in real vegetable samples.

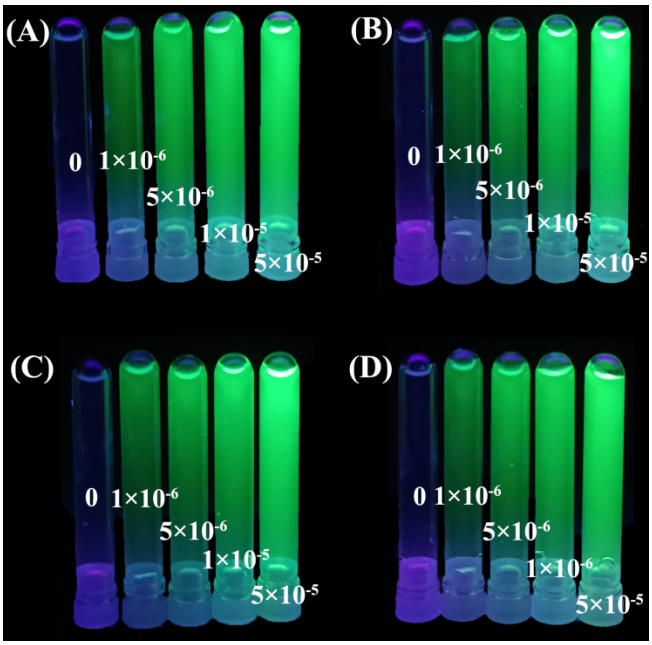

Figure 9. Extracts of different concentration of tricyclazole solution in the presence of the probe: (A) yam; (B) cabbage; (C) nectarine; (D) capsicum frutescens.

4. Conclusion

Herein, we have synthesized a fluorescent molecule HPy and have explored its host-guest interaction with the cucurbituril Q[8]. Our studies have revealed that the cavity of the Q[8] can encapsulate HPy and form an inclusion complex of formula HPy_2@Q[8]. The encapsulation of the HPy results in the quenching of the fluorescence emission. However, following the addition of the pesticide tricyclazole (TC), the latter can replace a HPy molecule in the Q[8] cavity, which results in the ternary complex TC@HPy@Q[8], and a sharp increase in the fluorescence intensity. The system is useful for TC detection given that none of the other 16 pesticides tested were able to turn on the fluorescence, and can be used to detect TC residues in real agricultural products. The simple strategy reported herein provides a perspective going forward for utilizing host-guest chemistry in the detection of other analytes of interest.

ACKNOWLEDGMENT

We thank the National Natural Science Foundation of China (NSFC no 21861011), and the Innovation Program for High-level Talents of Guizhou Province (No. 2016-5657) are gratefully acknowledged for financial support. CR thanks the EPSRC for an Overseas Travel Grant.

AUTHOR INFORMATION

Corresponding Authors

*E-mail: gyhxxiaoxin@163.com (Xiao X.).

REFERENCES

[1] Pundir C S, Chauhan N. Acetylcholinesterase inhibition-based biosensors for pesticide determination: A review. Anal Biochem. 2012; 429: 19-31. https://doi.org/10.1016/j.ab.2012.06.025.

[2] Gong J, Miao X, Zhou T, Zhang L. An enzymeless organophosphate pesticide sensor using Au nanoparticle-decorated graphene hybrid nanosheet as solid-phase extraction. Talanta. 2011; 85: 1344-1349. https://doi.org/10.1016/j.talanta.2011.06.016.

[3] Cortada C, Dos Reis L C, Vidal L, Llorc J, Canals A. Determination of cyclic and linear siloxanes in wastewater samples by ultrasound-assisted dispersive liquid–liquid microextraction followed by gas chromatography-mass spectrometry. Talanta. 2014; 120: 191-197. https://doi.org/10.1016/j.talanta.2013.11.042.

[4] Ko A Y, Rahman M M, Abd El-Aty A M, Jang J, Park J H, Cho S K, Shim J H. Development of a simple extraction and oxidation procedure for the residue analysis of imidacloprid and its metabolites in lettuce using gas chromatography. Food Chem. 2014; 148: 402-409. https://doi.org/10.1016/j.foodchem.2013.10.055.

[5] Vichapong J, Burakham R, Srijaranai S. Vortex-assisted surfactant-enhanced-emulsification liquid-liquid microextraction with solidification of floating organic droplet combined with HPLC for the determination of neonicotinoid pesticides. Talanta. 2013; 117: 221-228. https://doi.org/10.1016/j.talanta.2013.08.034.

[6] Qin L, Pan W, Rui C, Wei L, Wu Y J. Construction of genetically engineered bacteria that degrades organophosphorus pesticide residues and can be easily detected by the fluorescence. Environ Technol. 2014; 35: 556-561. https://doi.org/10.1080/09593330.2013.837936.

[7] Kanagaraj K, Affrose A, Sivakolunthu S, Pitchumani K. Highly selective fluorescent sensing of fenitrothion using per-6-amino-β-cyclodextrin:Eu(III) complex. Biosens Bioelectron. 2012; 35: 452-455. https://doi.org/10.1016/j.bios.2012.02.046.

[8] Zare-Shahabadi V, Abbasitabar F, Akhond M, Shamsipour. Simultaneous determination of chlorpyrifos and carbaryl by spectrophotometry and boosting partial least squares. J Brazil Chem Soc. 2013; 24: 1561-1569. https://doi.org/10.5935/0103-5053.20130197.

[9] Mitić S S, Živanović V V, Miletić G Ž, Grahovac Z M, Pecev E T. Determination of trace dimethoate in milk and river water by kinetic spectrophotometry using malachite green and

potassium periodate. J Anal Chem. 2012; 67: 284-289. https://doi.org/10.1134/S1061934812030082.

[10] Wang Y, Zhang L, Zhang S, Liu Z, Chen L. High Spatiotemporal Resolution Observation of Glutathione Hydropersulfides in Living Cells and Tissue via a Two-Photon Ratiometric Fluorescent Probe. Anal Chem, 2019; 91: 7812-7818. https://doi.org/10.1021/acs.analchem.9b01511.

[11] Wang Y, Han X, Zhang X, Zhang L, Chen L. A high selectivity fluorescent probe for hypoxia imaging in cells and tumor-bearing mice model. Analyst. 2020; 145: 1389-1395. https://doi.org/10.1039/C9AN02436K.

[12] Gao M, Zhang X, Wang Y, Liu Q, Yu F, Huang Y, Chen L. Sequential detection of superoxide anion and hydrogen polysulfides under hypoxic stress via a spectral-response-separated fluorescent probe functioned with a nitrobenzene derivative. Anal Chem. 2019; 91: 7774-7781. https://doi.org/10.1021/acs.analchem.9b01189.

[13] Huang Y, He N, Wang Y, Zhang L, Kang Q, Wang Y, Chen L. Detection of hypochlorous acid fluctuation via a selective near-infrared fluorescent probe in living cells and in vivo under hypoxic stress. J. Mater Chem B. 2019; 7: 2557-2564. https://doi.org/10.1039/C9TB00079H.

[14] Gao P L, Wang J G, Zheng M, Xie Z G. Lysosome targeting carbon dots-based fluorescent probe for monitoring pH changes in vitro and in vivo. Chem Eng J. 2020; 381: 122665. https://doi.org/10.1016/j.cej.2019.122665.

[15] Gu J P, Li X Q, Zhou Z, Liao R S, Gao J W, Tang Y P, Wang Q M. Synergistic regulation of effective detection for hypochlorite based on a dual-mode probe by employing aggregation induced emission (AIE) and intramolecular charge transfer (ICT) effects. Chem Eng J. 2019; 368: 157-164. https://doi.org/10.1016/j.cej.2019.02.175.

[16] Mir N, Heidari A, Beyzaei H, Mirkazehi-Rigi S, Karimi P. Detection of Hg^{2+} in aqueous solution by pyrazole derivative-functionalized Fe_3O_4@SiO_2 fluorescent probe. Chem Eng J. 2017; 327: 648-655. https://doi.org/10.1016/j.cej.2017.06.062.

[17] Wu H B, Shen J Y, Jiang X B, Liu X D, Sun X Y, Li J S, Han W Q, Mu Y, Wang L J. Bioaugmentation potential of a newly isolated strain Sphingomonas sp. NJUST37 for the treatment of wastewater containing highly toxic and recalcitrant tricyclazole. Bioresource Technology. 2018; 264: 98-105. https://doi.org/10.1016/j.biortech.2018.05.071.

[18] Pareja L, Martínez-Bueno M J, Cesio V, Heinzen H, Fernández-Alba A R. Trace analysis of pesticides in paddy field water by direct injection using liquid chromatography-quadrupole-linear ion trap-mass spectrometry. J Chromatogr A. 2011; 1218: 4790-4798. https://doi.org/10.1016/j.chroma.2011.02.044.

[19] Krieger M S, Cook W L, Kennard LM. Extraction of tricyclazole from soil and sediment with subcritical water. J. Agric. Food Chem. 2000; 48: 2178-2183. https://doi.org/10.1021/jf990626c.

[20] Padovani L, Capri E, Padovani C, Puglisi E, Trevisan M. Monitoring tricyclazole residues in rice paddy watersheds. Chemosphere. 2006; 62: 303-314. https://doi.org/10.1016/j.chemosphere.2005.05.025.

[21] Phong T K, Dang T, Yamazaki K, Takagi K, Watanabe H. Behavior of sprayed tricyclazole in rice paddy lysimeters. Chemosphere. 2009; 74: 1085-1089. https://doi.org/10.1016/j.chemosphere.2008.10.050.

[22] Zhang K, Mei Q S, Guan G J, Liu B H, Wang S H, Zhang Z P. Ligand replacement-induced fluorescence switch of quantum dots for ultrasensitive detection of organophosphorothioate pesticides. Anal. Chem. 2010; 82: 9579-9586. https://doi.org/10.1021/ac102531z.

[23] Bakirci H, Nau W M. Fluorescence regeneration as a signaling principle for choline and carnitine binding: a refined supramolecular sensor system based on a fluorescent azoalkane. Adv Funct Mater. 2006; 16: 237-242. https://doi.org/10.1002/adfm.200500219.

[24] Wen L, Sun Z, Han C, Imene B, Tian D, Li H B. Jiang, L. Fabrication of layer-by-layer assembled biomimetic nanochannels for highly sensitive acetylcholine sensing. Chem Eur J. 2013; 19: 7686-7690. https://doi.org/10.1002/chem.201300528.

[25] Guo D S, Uzunova V D, Su X, Liu Y, Nau W M. Operational calixarene-based fluorescent sensing systems for choline and acetylcholine and their application to enzymatic reactions. Chem Sci. 2011; 2: 1722-1734. https://doi.org/10.1039/C1SC00231G.

[26] Nau W M, Ghale G, Hennig A, Bakirci H, Bailey D M. Substrate-selective supramolecular tandem assays: monitoring enzyme inhibition of arginase and diamine oxidase by fluorescent dye displacement from calixarene and cucurbituril macrocycles. J Am Chem Soc. 2009; 131: 11558-11570. https://doi.org/10.1021/ja904165c.

[27] Chang Y X, Qiu Y Q, Du L M, Li C F, Guo M. Determination of ranitidine, nizatidine, and cimetidine by a sensitive fluorescent probe. Analyst. 2011; 136: 4168-4173. https://doi.org/10.1039/C1AN15078B.

[28] Wang G Q, Qin Y F, Du L M, Fu Y L. Supramolecular interaction of gliclazide with cucurbit[7]uril and its analytical application. Aust. J. Chem. 2013; 66: 701-710. http://dx.doi.org/10.1071/CH13087.

[29] Chang Y X, Duan X C, Zhang X M, Liu F, Du L M. A new fluorometric method for the determination of oxaliplatin based on cucurbit[7]uril supramolecular interaction. Aust J Chem. 2016; 70: 667-673. http://dx.doi.org/10.1071/CH16398.

[30] Shan P H, Zhao J, Deng X Y, Lin R L, Bian B, Tao Z, Xiao X, Liu J X. Selective recognition and determination of phenylalanine by a fluorescent probe based on cucurbit[8]uril and palmatine. Analy Chim. Acta. 2020; 1104: 164-171. https://doi.org/10.1016/j.aca.2020.01.007.

[31] Masson E, Ling X X, Joseph R, Kyeremeh-Mensah L, Lu X Y. Cucurbituril chemistry: a tale of supramolecular success. RSC Advances. 2012; 2: 1213-1247. https://doi.org/10.1039/C1RA00768H.

[32] Ni X L, Xiao X, Cong H, Liang L L, Chen K, Cheng X J, Ji N N, Zhu Q J, Xue S F, Tao Z. Cucurbit[n]uril-based coordination chemistry: from simple coordination complexes to novel poly-dimensional coordination polymers. Chem Soc Rev, 2013; 42: 9480-9508. https://doi.org/10.1039/C3CS60261C.

[33] Kaifer A E. Toward Reversible Control of Cucurbit[n]uril Complexes. Acc Chem Res. 2014; 47: 2160-2167. https://doi.org/10.1021/ar5001204.

[34] Assaf K I, Nau W M. Cucurbiturils: from synthesis to high-affinity binding and catalysis. Chem Soc Rev. 2015; 44: 394-418. https://doi.org/10.1039/C4CS00273C.

[35] Shetty D, Khedkar J K, Parkad K M, Kim K. Can we beat the biotin-avidin pair?:cucurbit[7]uril-based ultrahigh affinity host–guest complexes and their applications. Chem Soc Rev. 2015; 44: 8747-8761. https://doi.org/10.1039/C5CS00631G.

[36] Barrow S J, Kasera S M, Rowland J, Barrio J, Scherman O A. Cucurbituril-Based Molecular Recognition. Chem Rev. 2015; 115: 12320-12406. https://doi.org/10.1021/acs.chemrev.5b00341.

[37] Liu M, Chen L X, Shan P H, Lian C J, Zhang Z H, Zhang Y Q, Tao Z, Xiao X. Pyridine Detection Using Supramolecular Organic Frameworks Incorporating Cucurbit[10]uril. ACS Appl Mater Inter. 2021; 13: 7434-7442. https://doi.org/10.1021/acsami.0c20292.

[38] Yang D, Liu M, Xiao X, Tao Z, Redshaw C. Polymeric self-assembled cucurbit[n]urils: Synthesis, structures and applications. Coordin Chem Rev. 2021; 434: 213733. https://doi.org/10.1016/j.ccr.2020.213733.

[39] Liu M, Yang M X, Yao Y Q, Zhang Y J, Zhang Y Q, Tao Z, Zhu Q J, Wei G, Bian B, Xiao X. Specific recognition of formaldehyde by a cucurbit[10]uril-based porous supramolecular assembly incorporating adsorbed 1,8-diaminonaphthalene. J Mater Chem C. 2019; 7: 1597-1603. https://doi.org/10.1039/C8TC06339G.

[40] Liu M, Kan J L, Yao Y Q, Zhang Y Q, Bian B, Tao Z, Zhu Q J, Xiao X. Facile preparation and application of luminescent cucurbit[10]uril-based porous supramolecular frameworks. Sensor Actuat B: Chem. 2019; 283: 290-297. https://doi.org/10.1016/j.snb.2018.12.024.

[41] Gao R H, Chen L X, Chen K, Tao Z, Xiao X. Development of hydroxylated cucurbit[n]urils, their derivatives and potential applications. Coordin Chem Rev. 2017; 348: 1-24. https://doi.org/10.1016/j.ccr.2017.07.017.

[42] Lazar A I, Biedermann F, Mustafina K R, Assaf K I, Hennig A, Nau W M. Nanomolar binding of steroids to cucurbit[n]urils: selectivity and applications. J Am Chem Soc. 2016; 138: 13022-13029. https://doi.org/10.1021/jacs.6b07655.

[43] Yao F H, Liu H L, Wang G Q, Du L M, Yin X F, Fu Y L. Determination of paraquat in water samples using a sensitive fluorescent probe titration method. Journal of Environmental Sciences. 2013; 25: 1245-1251. https://doi.org/10.1016/S1001-0742(12)60124-7.

[44] Sun S G, Li F S, Liu F Y, Wang J T, Peng X J. Fluorescence detecting of paraquat using host-guest chemistry with cucurbit[8]uril. Scientific Reports, 2014; 4: 3570. https://doi.org/10.1038/srep03570.

[45] Xing X, Zhou Y, Sun J, Tang D, Kai W. Determinat.on of paraquat by cucurbit[7]uril sensitized fluorescence quenching method. Analytical Letters. 2013; 46: 694-705. https://doi.org/10.1080/00032719.2012.729240.

[46] Pozo MD, Hernández L, Quintana C. A selective spectrofluorimetric method for carbendazim determination in oranges involving inclusion-complex formation with

cucurbit[7]uril. Talanta, 2010; 81:1542-1546. https://doi.org/10.1016/j.talanta.2010.02.066.

[47] Xu W T, Luo Y, Zhao W W, Liu, M, Luo G Y, Fan Y, Lin R L, Tao Z, Xiao X, Liu J X. Detecting Pesticide Dodine by Displacement of Fluorescent Acridine from Cucurbit[10]uril Macrocycle. J Agric Food Chem, 2021; 69: 584-591. https://doi.org/10.1021/acs.jafc.0c05577.

[48] Luo Y, Zhang W, Liu M, Zhao J, Fan Y, Bian B, Tao Z, Xiao X. A supramolecular fluorescent probe based on cucurbit[10]uril for sensing the pesticide dodine. Chinese Chem. Lett. 2021; 32: 367-370. https://doi.org/10.1016/j.cclet.2020.02.023.

[49] Kim S J, Jung I S, Kim S Y, Lee E, Kim J, Sakamoto S, Yamaguchi K, Kim K. Macrocycles within macrocycles: cyclen, cyclam, and their transition metal complexes encapsulated in cucurbit[8]uril. J Am Chem Soc, 2000; 122: 540-541. https://doi.org/10.1002/1521-3773(20010601)40:11<2119::AID-ANIE2119>3.0.CO;2-4.